

ments available, but the agreement with experiment is good. For point defects, where the calculations are expected to be less reliable, there are many measurements, and the agreement with experiment is fair and better than might have been expected. For example, the calculations for the effects of Freknel defects on the bulk modulus of LiF are found to be closer to experimental results than are other available estimates. A number of models for point defects are discussed, but no entirely successful model for all point defects is found. It is found, however, that a simple GV form for the energy can be used to estimate the order of magnitude of the changes due to most kinds of defects.

The present calculation of the volume change produced by dislocations predicts that dislocations in certain ionic crystals including LiF may have hollow cores in agreement with the conclusions from measurements of pipe diffusion in LiF. It is predicted that this effect will be absent in certain alkali halides. The calculations suggest that the formation entropies for vacan-

cies in some metals might be larger by 1 to 2 entropy units than has previously been supposed. A discussion of high-temperature thermal expansion and specific heat measurements for metals shows that most previous analyses of these measurements have overestimated the effects due to the thermal equilibrium defects present and underestimated the effects of lattice anharmonicity.

ACKNOWLEDGMENTS

We are indebted to Professor C. P. Flynn, Professor R. O. Simmons, and Professor J. S. Koehler for their comments and opinions in relation to the present calculation and for bringing a number of useful references to our attention. We would like to thank Professor D. Gerlich for many discussions regarding the LiF elastic constant measurements, and Dr. Tetsuro Suzuki and R. L. Marhsall for discussions relating to the elasticity calculations.

Magnetoreflexion Studies in Arsenic*†

MARTIN MALTZ‡§

*Department of Electrical Engineering and Center for Materials Science and Engineering,
Massachusetts Institute of Technology, Cambridge, Massachusetts 02139*

AND

M. S. DRESSELHAUS‡

*Department of Electrical Engineering, Center for Materials Science and Engineering,
and Lincoln Laboratory, || Massachusetts Institute of Technology, Cambridge, Massachusetts 02139*

(Received 17 January 1969)

An infrared magnetoreflexion study has been made of the trigonal face of single-crystal arsenic. Oscillations of very large amplitude have been observed with a line shape quite unlike any previously reported. It has been found that the complicated line shape can be understood by assuming that the oscillations are associated with interband transitions between a pair of coupled bands at a point of low symmetry (point Q) in the Brillouin zone. On the basis of this assumption, the data can be interpreted to obtain various band parameters such as the energy gap and the cyclotron effective mass. Some observed nonparabolic effects can also be explained. The magnetoreflexion data for the trigonal face are found to be consistent with Lin and Falicov's arsenic energy-band model.

I. INTRODUCTION

RECENT experimental¹⁻⁴ and theoretical⁵ studies of the semimetal arsenic have greatly advanced our understanding of the band structure of this material.

In particular, the band-structure calculation by Lin and Falicov⁵ for arsenic using the pseudopotential technique yields a Fermi surface whose shape is in reasonable

Massachusetts Institute of Technology, Cambridge, Mass., supported by the U. S. Air Force Office of Scientific Research.

§ Present address: Xerox Corporation, Rochester, N. Y.

|| Operated with support from the U. S. Air Force.

¹ M. G. Priestley, L. R. Windmiller, J. B. Ketterson, and Y. Eckstein, *Phys. Rev.* **154**, 671 (1967).

² J. Vanderkooy and W. R. Datars, *Phys. Rev.* **156**, 671 (1967).

³ W. R. Datars and J. Vanderkooy, *J. Phys. Soc. Japan Suppl.* **21**, 657 (1966).

⁴ C. Chung-Sen Ih, Ph.D. thesis, University of Pennsylvania, 1966 (unpublished).

⁵ P. J. Lin and L. M. Falicov, *Phys. Rev.* **142**, 441 (1966).

* This paper is based on a thesis submitted by one of the authors (M.M.) in partial fulfillment for the Ph.D. degree in the Electrical Engineering Department, Massachusetts Institute of Technology, Cambridge, Mass., 1968 (unpublished).

† Work supported in part by the U. S. Office of Naval Research, under Contract No. Nonr-1841(72), and Advanced Research Projects Agency, under Contract No. SD-90.

‡ Visiting scientist, Francis Bitter National Magnet Laboratory,

agreement with a large body of experimental data. Since almost no experimental information has been available about the band structure away from the Fermi level, we thought that it would be interesting to study arsenic using the magnetoreflexion technique, which gives such information, and to use our experimental results to explore the validity of the Lin-Falicov model away from the Fermi surface. The magnetoreflexion results which we obtained with magnetic fields parallel to the binary and bisectrix crystalline axes were presented in a previous publication,⁶ and indicate certain departures from the predictions of the Lin-Falicov model. In this paper, we discuss oscillations in the magnetoreflexivity which are observed with the magnetic field along the trigonal crystalline axis. These oscillations can be interpreted within the framework of the band model of Lin and Falicov, and are identified with electronic transitions between the bands associated with what have come to be called the γ carriers.¹

In exploring the agreement between theory and experiment for this case, we have considered not only the energy gap and the cyclotron effective mass implied by the experimentally observed oscillations, but have considered the amplitudes and phases of the oscillations as well. The analysis is complicated, however, by the fact that the critical point seems to lie along a line of low symmetry (the Q axis) in the Brillouin zone. It has been found, however, that the magnetoreflexion technique is an effective tool for studying energy bands even about such low symmetry points. At these critical points, the magnetoreflexion spectra for interband Landau-level transitions is considerably more complicated than the spectra expected at critical points of higher symmetry. These complications can, however, be understood on the basis of a simple model. This model can then be used to determine the band parameters for arsenic about the critical point of low symmetry.

In Sec. II we begin our discussion by describing previous experimental and theoretical studies which are relevant to an understanding of the electronic band structure of arsenic. In Sec. III we present and interpret the results of the magnetoreflexion experiment for the case where the magnetic field is parallel to the trigonal axis of the crystal. Finally, in Sec. IV we summarize the results of all of our magnetoreflexion studies of arsenic.

II. BACKGROUND

The first detailed information about the electronic band structure of arsenic was obtained in a set of de Haas-van Alphen (dHvA) experiments performed by Berlincourt.⁷ Two sets of carriers were observed which we call the α and γ carriers using the notation

⁶ Martin Maltz and M. S. Dresselhaus, Phys. Rev. Letters **20**, 919 (1968).

⁷ T. G. Berlincourt, Phys. Rev. **99**, 1716 (1955).

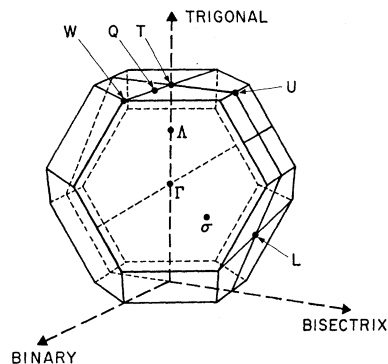


FIG. 1. Brillouin zone for the group-A7 crystalline structure, using the notation of Lin and Falicov. The mirror planes σ contain the Γ , T , and L points.

of Priestley *et al.*^{1,8} The α carriers were found to lie in either three or six pockets, with the center of each pocket in one of the mirror planes. (See the Brillouin zone of Fig. 1.) The γ pockets were found to have a smaller cross-sectional Fermi-surface area than the α pockets, but their number and placement in the Brillouin zone were not definitely established. In this work⁷ the effective masses for both the α and γ carriers were found by studying the temperature dependence of the amplitude of the dHvA oscillations.

Since the total hole and electron charge concentration must be equal in a pure semimetal, the results of Berlincourt indicated that there was at least one more carrier yet to be found. dHvA-type oscillations in the ultrasonic attenuation and differential susceptibility, observed in 1965 by Shapira and Williamson⁹ were identified with this carrier, which we call the β carrier,¹⁰ in accordance with the notation of Priestley *et al.*¹ These carriers were also found to lie in either three or six pockets, with the center of each pocket in one of the mirror planes (Fig. 1). In addition, the β pockets were found to be roughly ellipsoidal in shape, while the α pockets displayed some nonellipsoidal behavior. Since the temperature dependence of the dHvA amplitudes was not reported by Shapira and Williamson,⁹ no information about the effective masses for the β carriers was available. Ketterson and Eckstein¹¹ also carried out an ultrasonic magnetoattenuation experiment and observed quantum oscillations associated with the three carrier types.¹² Their results are consistent with the work of Shapira and Williamson.⁹ Ketterson and Eckstein did not report the temperature dependence of the oscillations.

⁸ Berlincourt used a different notation himself. Our γ and α carriers correspond to his α and β carriers, respectively.

⁹ Y. Shapira and S. J. Williamson, Phys. Letters **14**, 73 (1965).

¹⁰ This was called the γ carrier by Shapira and Williamson (Ref. 9). For the other two carriers these authors used the notation of Berlincourt (Ref. 7).

¹¹ J. B. Ketterson and Y. Eckstein, Phys. Rev. **140**, A1355 (1965).

¹² In Ref. 11, the notation for the α and β carriers is that of Ref. 5 and the present work.

In 1965, an attempt was made by Tanuma *et al.* to identify the sign of the charge for the α , β , and γ carriers by studying the effect of doping on the dHvA periods.¹³ The results, however, were inconclusive.

At about the same time, Datars and Vanderkooy³ studied arsenic using Azbel-Kaner cyclotron resonance in the extreme anomalous limit. The measured cyclotron effective masses agreed reasonably well with those found by Berlincourt⁷ for the α carriers.

In addition to this experimental work, a band-structure calculation for arsenic was carried out by Golin, using a self-consistent orthogonalized-plane-wave (OPW) method.¹⁴ No fit to the experimental data at the Fermi surface could be achieved with Golin's bands. This is not surprising in view of the recent observation⁶ of band gaps near the Fermi level which are smaller than the estimated calculational uncertainty.¹⁴ More recently, Lin and Falicov⁵ carried out a pseudopotential calculation of the arsenic energy bands, and in this case a good fit to the experimental data at the Fermi surface was obtained by adjustment of certain parameters characterizing the pseudopotential model. These results have therefore served as a guide to the interpretation of all the subsequent work.

The Lin-Falicov band model identifies the β carriers as electrons, which lie in three roughly ellipsoidal pockets centered about the L points in the Brillouin zone. The α and γ carriers correspond to parts of the multiply connected hole surface shown in Fig. 2. The α carriers lie in the six large turnip shaped pockets, and the γ carriers are in the long, narrow necks which connect them. Note that although holes occur near the T point, this model predicts no carriers at T , or in fact anywhere along the ΓT or A or trigonal axis. In Fig. 3(a) we show a particularly interesting aspect of the band structure which was used to construct the Lin-Falicov

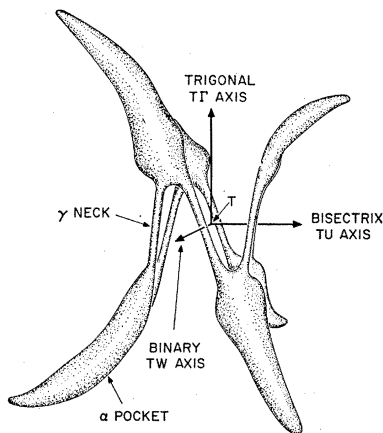


FIG. 2. Arsenic-hole Fermi surface, as determined by Lin and Falicov (Ref. 5).

¹³ S. Tanuma, Y. Ishizawa, and S. Ishiguro, *J. Phys. Soc. Japan Suppl.* **21**, 662 (1966).

¹⁴ S. Golin, *Phys. Rev.* **140**, A993 (1965).

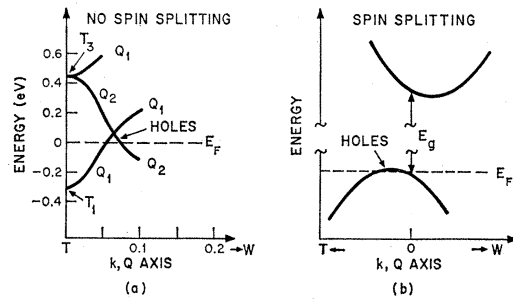


FIG. 3. Energy bands along the Q axis near the γ carriers. (a) The energy bands as determined by Lin and Falicov. The spin-orbit interaction has not been considered. The k vector is measured in a.u. (Ref. 27). (b) A magnified view of the region near the accidental degeneracy in (a) with spin-orbit coupling taken into account. The displacement between the band extrema is arbitrary. The k vector is measured from the extremum in the energy band separation.

Fermi surface.⁵ In this figure, we see that along the Q (i.e., TW or binary) axis, close to T , there is an accidental crossover degeneracy, giving rise to the hole carriers of the γ necks. If spin-orbit coupling had been considered, this degeneracy would be lifted as shown by the band gap in Fig. 3(b). We have identified the oscillations in the magnetorefectivity observed with the magnetic field along the trigonal crystalline axis with interband transitions across this spin-orbit energy gap. The extrema of the two bands need not occur at the same point in the Brillouin zone because the only symmetry operation at a general point along the Q axis is a twofold rotation about this axis, and therefore inversion symmetry is lacking. To say this more precisely, if the k_x direction is taken along the Q axis, then the k_x values for the two-band extrema may differ, but the k_y and k_z values for bisectrix and trigonal directions will be the same for the two-band extrema. In this figure, the band gap E_g is taken at the k point of minimum energy separation.

The Lin-Falicov band model has been applied to the interpretation of a number of experimental studies on the arsenic Fermi surface. A summary of the experimental results is given in Table I. Wherever possible in this table, a comparison has been made between the experimental results and the theory of Lin and Falicov.⁵ In particular, it is found that the dHvA studies by Priestley *et al.*¹ and of Vanderkooy and Datars² tend to support the general topology of the Lin-Falicov band model, as do the Azbel-Kaner cyclotron resonance studies of Datars and Vanderkooy³ and of Chung-Sen Ih.⁴ However, the effective masses which they measure are quite different from those predicted from the Lin-Falicov band model, indicating that the model may not be accurate away from the Fermi surface. Therefore, optical data which provide information about energy bands away from the Fermi surface are of great interest.

The first set of optical experiments were carried out

TABLE I. Fermi-surface data for arsenic.

Quantity	Experiment	Theory
α carriers		
Fermi energy	0.180 eV ^a	0.361 eV ^b
Carrier density/ellipsoid	$3.9 \times 10^{19} \text{ cm}^{-3a}$	
Tilt angle (min. area)	37.25° ^a	44° ^b
Area ^c (min. area)	3.981×10^{-3a}	
m^* (min. area)	0.096 ^a	
β carriers		
Fermi energy	0.190 eV ^a	0.367 eV ^b
Carrier density/ellipsoid	$7.07 \times 10^{19} \text{ cm}^{-3a}$	
Tilt angle (min. area)	86.4° ^a	80° ^b
Area ^d (min. area)	0.005695 ^a	0.0055 ^{b,e}
m^* (min. area)	0.127 ^d	
Area, $\circ \mathbf{H} \parallel \text{bin}$, principal ellipsoid	0.02 ^a	0.016 ^b
m^* , $\mathbf{H} \parallel \text{bin}$, principal ellipsoid	0.404 ^d	
m^* , $\mathbf{H} \parallel \text{bin}$, nonprincipal ellipsoid	0.150 ^d	0.11 ^b
Area, $\circ \mathbf{H} \parallel \text{trig}$,	0.021 ^a	0.018 ^b
m^* , $\mathbf{H} \parallel \text{trig}$,	0.361 ^d	
m^* , $\mathbf{H} \parallel \text{bis}$, nonprincipal ellipsoid	0.130 ^d	
γ carriers		
Fermi level	0.011 eV ^a	
Area, $\circ \mathbf{H} \parallel \text{trig}$	6.9×10^{-5a}	$6.9 \times 10^{-5b,f}$
Tilt angle	-10° ^a	-11° ^b
m^* , $\mathbf{H} \parallel \text{trig}$	0.028, ^a 0.0269 ^g	
Reciprocal effective-mass tensor for γ carriers. ^h		

$$\alpha = - \begin{pmatrix} 23.9 & 0 & 0 \\ 0 & 59.5 & 10.3 \\ 0 & 10.3 & 1.22 \end{pmatrix}$$

- ^a Priestley *et al.* (Ref. 1).
^b Lin and Falicov (Ref. 5).
^c Fermi-surface cross-sectional area is measured in a.u. (Ref. 27).
^d C. C.-S. Ih (Ref. 4).
^e Lin and Falicov (Ref. 5) adjusted electron Fermi level to fit this area measured by Priestley *et al.* (Ref. 1).
^f Lin and Falicov (Ref. 5) adjusted hole Fermi level to fit this area measured by Priestley *et al.* (Ref. 1).
^g Present work.
^h Derived from orientation dependence of dHvA periods measured by Priestley *et al.* (Ref. 1) requiring m^* for $\mathbf{H} \parallel \text{trig}$ to be 0.028.

by Cardona and Greenaway.¹⁵ In these experiments, structure was observed in the reflectivity in the photon energy range between 1 and 23 eV. These data, therefore, provide almost no information about the infrared, which is the region of the spectrum most likely to contain detailed information about the band structure near the Fermi surface. Precisely this range of photon energies was explored in a recently reported series of infrared magnetorefectivity experiments performed with the magnetic field along the binary and bisectrix crystalline axes.⁶ The observed magnetorefectivity oscillations were interpreted as being associated with an interband transition across a small, direct energy band gap of 0.346 eV between bands having either the T_2 and $T_{1'}$ or the $T_{2'}$ and T_1 symmetries, using the symmetry notation of the Lin-Falicov calculation.⁵ Unfortunately, this calculation does not display any small direct gaps between bands of the symmetries required by the magnetorefectivity experiment.⁶

¹⁵ M. Cardona and D. L. Greenaway, Phys. Rev. **133**, A1685 (1964).

III. MAGNETOREFLECTION EXPERIMENTS—TRIGONAL SAMPLE ORIENTATION

In contrast with the previous magnetoreflexion study of arsenic,⁶ the work reported here was carried out with the magnetic field along the trigonal crystalline axis. In this case, a different series of oscillations in the magnetoreflexivity is observed and this series can be interpreted within the framework of the band model of Lin and Falicov.⁵ No oscillations associated with the band gap of 0.346 eV have been found for this orientation of magnetic field.

In our experiments, the optical reflectivity of a liquid-helium-cooled single-crystal sample is measured as a function of magnetic field and photon energy in the Faraday geometry (magnetic field and optical propagation vector parallel to each other). A detailed description of the equipment used to make the measurements, and the sample preparation techniques,

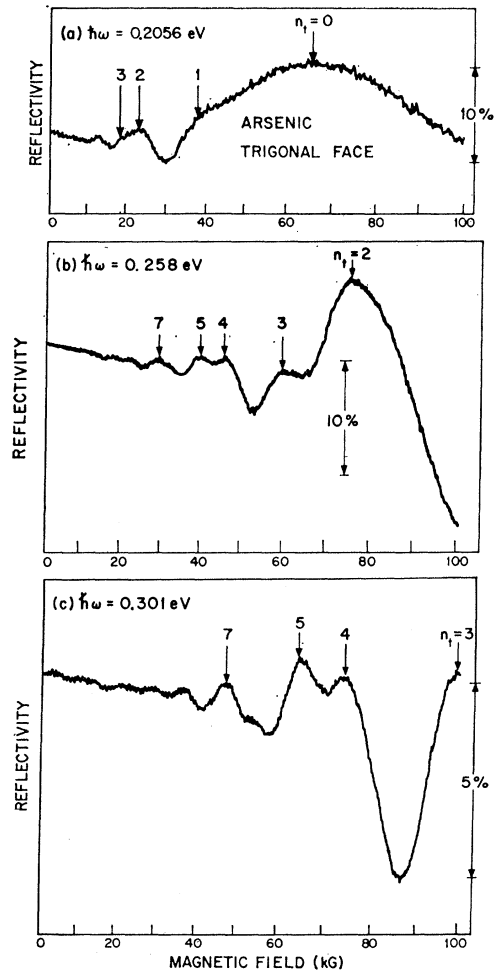


FIG. 4. Magnetoreflexivity recorder traces of arsenic for the trigonal face. The amplitude calibration is given as a percentage of the zero-field reflectivity. The n_i quantum number labels the resonant peaks. (a) Photon energy = 0.2056 eV; (b) photon energy = 0.258 eV; and (c) photon energy = 0.301 eV.

has been given in a previous publication⁶ and is identical with the experimental procedures used for the binary and bisectrix sample orientations, except that the trigonal face was prepared by cleaving.

Three representative experimental traces, taken at different photon energies, are displayed in Fig. 4. These oscillations exhibit many peculiarities. First of all, their amplitude is very large; larger, in fact, than the amplitude of the oscillations observed for any other semimetal.¹⁵⁻¹⁸ Not only are these oscillations observed at liquid-helium temperatures, but also at liquid-nitrogen temperatures, reduced in amplitude by a factor of only $\frac{1}{3}$. One reason for the large amplitude of these oscillations is that the photon energies of Fig. 4 occur near the plasma frequency of the material ($\hbar\omega_p=0.26$ eV).¹⁹ At this frequency the free carrier and interband contributions to the dielectric constant are nearly cancelled out by the contribution due to the core polarization, so that any oscillatory effects in the dielectric constant are greatly enhanced. Other reasons for the large magnitude of these oscillations are discussed later in this paper.

The line shape of these unusually large oscillations is quite unlike any line shape which has previously been reported for either a semiconductor or semimetal.²⁰ In particular, for a given photon energy an unusual variation of the line shape and oscillation amplitude is observed as a function of n_t , an index used to label the resonant structures (Fig. 4). It is found that the amplitude of the n_t =even oscillations decreases with increasing n_t much more rapidly than does the amplitude of the n_t =odd oscillations.²¹ It is further found that the general line shape of an oscillation with a particular value of n_t does not vary as a function of photon energy. In other words, the reflectivity and magnetic field scales of the curves seem to change with photon energy, while the relative shapes of the oscillations remain constant.

Let us ignore, for the moment, these peculiarities in the line shape and proceed in the traditional way, by plotting the resonance fields as a function of photon energy in the "fan chart" of Fig. 5. In constructing this figure, a resonance field is experimentally defined as the field at the peak in the reflectivity. By looking at this fan chart, it is clear that the observed oscillations are associated with interband transitions across a single

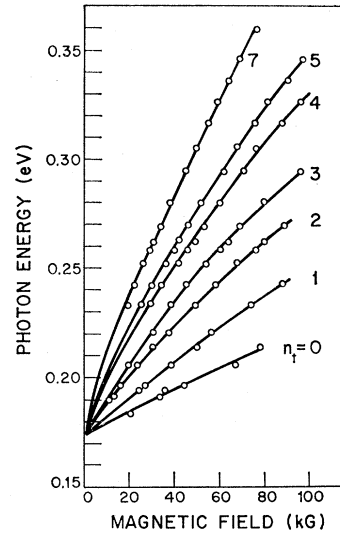


FIG. 5. Summary of the observed peaks in the reflectivity for the trigonal face of arsenic.

band gap of about 0.175 eV. Also, it is found that the lines through the experimental points on this fan chart are relatively straight, so that we can assume that the energy bands are essentially parabolic for the energy range over which oscillations have been observed.²⁰ We further note that, for a given magnetic field, the large energy separations between adjacent resonance loci indicate a small reduced cyclotron effective mass for the bands involved in the transitions. A small effective mass generally indicates a strong coupling between the bands in the two directions perpendicular to the magnetic field (i.e., the binary, or x , and the bisectrix, or y , directions) and therefore the bands are expected to have nearly equal and opposite curvatures in these directions. These arguments imply that the cyclotron effective masses for these two bands are equal, so that ignoring spin, one might expect that the resonant fields and photon energies would be related by the simple expression

$$\hbar\omega_{\text{res}} = E_g + \beta_0 H_{\text{res}} (n_c + n_v + 1) / m_c^*, \quad (1)$$

where

$$\beta_0 = |e| \hbar / (m_0 c). \quad (2)$$

Here m_c^* is the dimensionless cyclotron effective mass for either band, and n_c and n_v are the Landau-level indices for any coupled conduction and valence band Landau levels. If we now assume the traditional inter-Landau-level, interband transition selection rule, $\Delta n = 0$, then Eq. (1) reduces to

$$\hbar\omega_{\text{res}} = E_g + 2\beta_0 H_{\text{res}} (n - \psi) / m_c^*, \quad (3)$$

with the phase $\psi = -\frac{1}{2}$ and $n = \text{integer}$. From this expression we would conclude that at constant photon energy the oscillations should be periodic in $1/H$, with a phase of $-\frac{1}{2}$. In order to test the validity of this

¹⁶ R. N. Brown, J. G. Mavroides, and B. Lax, Phys. Rev. **129**, 2055 (1963).

¹⁷ M. S. Dresselhaus and J. G. Mavroides, IBM J. Res. Develop. **8**, 262 (1964).

¹⁸ M. S. Dresselhaus and J. G. Mavroides, Phys. Rev. Letters **14**, 259 (1965).

¹⁹ M. Maltz, thesis, Massachusetts Institute of Technology, 1968 (unpublished).

²⁰ B. Lax and J. G. Mavroides, *Optical Properties of III-V Compounds*, edited by R. K. Willardson and A. C. Beer (Academic Press Inc., New York, 1967), Vol. III.

²¹ The n_t =even oscillation amplitudes decrease so rapidly with increasing n_t that we were not able to clearly observe the $n_t=6$ oscillation at all. This oscillation was observed, however, by Dr. S. Iwasa of MIT in a high resolution magnetoreflexion experiment, using a laser source.

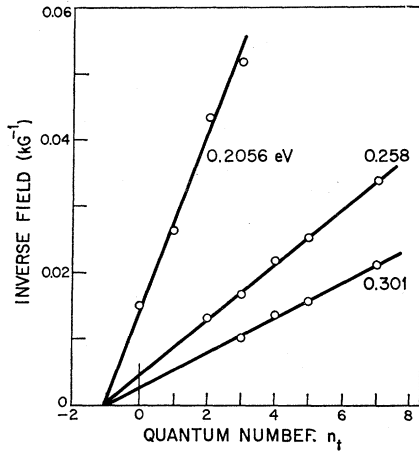


FIG. 6. Inverse resonant fields as a function of the quantum number n_t at three different photon energies.

selection rule we have plotted in Fig. 6 the inverse resonant fields as a function of n_t for the three photon energies of Fig. 4, and have found that the expected periodicity is present, but that the n_t axis intercept, or phase, is -1 .

The simplest way to understand this peculiar phase²² is to assume that in this case there is some mechanism which breaks down the customary $\Delta n=0$ interband, inter-Landau-level selection rule. With a breakdown in selection rule, n_c and n_v could have any values, and the resonant fields and photon energies would be related by the expression

$$\hbar\omega_{\text{res}} = E_g + \beta_0 H_{\text{res}}(n_t + 1)/m_c^*, \quad (4)$$

where we have defined $n_t = n_c + n_v$. From this equation, we therefore expect oscillations periodic in $1/H$, with a period P given by

$$P = \beta_0 / [m_c^*(\hbar\omega - E_g)], \quad (5)$$

and a phase of -1 , in agreement with the phase of the observed oscillations. Furthermore, we note that the normally allowed $n_v = n_c$ inter-Landau-level transition only contributes to the $n_t = \text{even}$ oscillations, and not at all to the $n_t = \text{odd}$ ones. Therefore, this model can be expected to yield quite different line shapes for the $n_t = \text{even}$ and $n_t = \text{odd}$ oscillations; and this is, in fact, observed. Before discussing the mechanism responsible for the breakdown in the selection rule, we shall complete the discussion of the analysis of the magneto-reflection spectrum. First of all, we note that Eq. (5) predicts a linear dependence of $1/P$ on the photon energy, with a slope of

$$\partial(1/P)/\partial(\hbar\omega) = m_c^*/\beta_0, \quad (6)$$

and an energy axis intercept of E_g . To find m_c^* and E_g we have therefore plotted in Fig. 7 the photon energy

as a function of $1/P$ for all of the data we have obtained. Fitting the low-energy data with a straight line, we obtain an energy gap of $E_g = 0.177 \pm 0.005$ eV, and from the slope of the line we find that $m_c^* = 0.031 \pm 0.003$. At higher photon energies the departure of the points from the straight line indicates that the bands have a small, but noticeable amount of nonparabolic character.

The small value that we have found for m_c^* is consistent with our assumption that the two bands under consideration interact strongly with each other in the x and y directions (though this is not necessarily true along the z , or trigonal, direction). It therefore seems reasonable to assume that for the x and y directions we may neglect the interaction of our two bands with the other bands nearby, thus implying equal and opposite band curvatures in the x and y directions. The assumption that the two bands interact only with each other, however, is the essential assumption made in constructing the nonparabolic two-band model of Lax,¹⁶ Kane,²³ and Cohen.²⁴ In order to apply such a nonparabolic band model to the arsenic problem, we further assume that the mechanism which produces a breakdown in the customary $\Delta n=0$ selection rule represents a small perturbation on the form of the two-band energy-momentum dispersion relations. To test the validity of these assumptions, we attempted to describe the nonparabolic nature of the arsenic bands by the strongly coupled two-band model, according to which the energy-momentum relation for the conduction and valence bands is

$$E = \pm [\frac{1}{4}E_g^2 + \frac{1}{2}E_g\hbar^2\mathbf{k}\cdot\boldsymbol{\alpha}\cdot\mathbf{k}/m_0]^{1/2}, \quad (7)$$

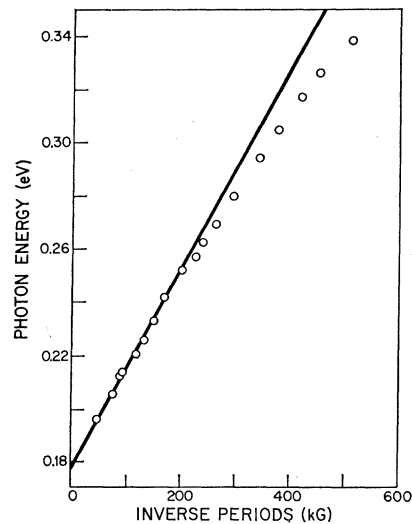


FIG. 7. Inverse periods (taken from graphs such as Fig. 6) as a function of photon energy. The solid line is a straight-line fit (parabolic-band model) to the low-energy data.

²² For example, the phase is $\psi = -\frac{1}{2}$ for bismuth, and also for arsenic with the magnetic field perpendicular to the trigonal axis.

²³ E. O. Kane, J. Phys. Chem. Solids **1**, 249 (1957).

²⁴ M. H. Cohen, Phys. Rev. **121**, 387 (1961).

in which α is the reciprocal effective mass tensor at the critical point.²⁵

Upon analysis of the magnetoreflexion data in arsenic we will find that m^* , the cyclotron effective mass at the band extremum, is of the order of 0.03, so that at the highest magnetic fields available $\beta_0 H/m^*$ is only about 0.03 eV. Our experiments are therefore performed in the small field limit, where $E_g \gg \beta_0 H/m^*$, and in this limit it may be shown from Eq. (7) that the inverse periods are given by

$$1/P = \frac{1}{2} m^* [(\hbar\omega)^2 - E_g^2] / \beta_0 E_g. \quad (8)$$

This expression is most accurate for the $\Delta n=0$ transition and is approximately valid for transitions with small values of Δn . In the Appendix we discuss a mechanism suggested by the symmetry properties of the critical point which can produce a breakdown in the selection rule $\Delta n=0$. In order to use Eq. (8) to find the parameters E_g and m^* , we have plotted $(\hbar\omega)^2$ as a function of $1/P$ in Fig. 8. We find that the data points do fall on a straight line, thereby justifying the assumption of a two-band model for the x and y directions. From the $(\hbar\omega)^2$ -axis intercept we find that $E_g = 0.172 \pm 0.003$ eV, and from the slope of the line we obtain $m^* = 0.0238$. It should be noted that the cyclotron effective mass m_c^* at energy E' is related to the effective-mass parameter m^* according to

$$m_c^* = m^* (2E' + E_g) / E_g, \quad (9)$$

where the energy E' is measured from the energy extremum of one of the bands.

Upon comparing these results with the dHvA and cyclotron resonance measurements which have been reported in the literature (see Table I), we note that the only values of m_c^* of such small magnitude are the values measured for the γ carrier with the magnetic field along the z axis. Using the Fermi level reported by Priestley *et al.*¹ ($E_f = 0.011$ eV as measured from the maximum energy of the hole band) and Eq. (9), a value of 0.0269 for m_c^* at the Fermi surface is obtained, assuming that the holes of the γ necks are associated with one of the bands under discussion. Since this value agrees very well with the value of 0.028 measured by Priestley *et al.*,¹ it seems very reasonable to assume that one of our bands is, in fact, associated with these carriers.

Since there are carriers associated with one of the bands, there should be a Fermi level cutoff in the data at the energy below which Landau-level transitions cannot occur because of the unoccupied states in the valence band. Unfortunately, however, we have not been able to decide experimentally whether or not such a cutoff exists. The essential difficulty is due to the finite resolution and signal-to-noise ratio of our instru-

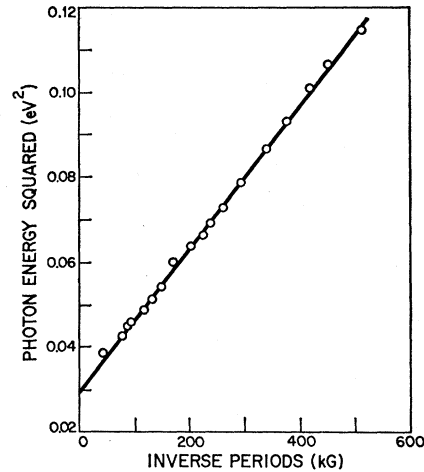


Fig. 8. Inverse periods as a function of the photon energy squared (the two-band model). The solid line is a straight-line fit to the data.

ment, which results in an inability to see any sharp structure in the arsenic magnetoreflexivity at photon energies below 0.190 eV. Therefore, although we can be certain that there is no cutoff above this photon energy, we cannot conclude that there is no cutoff below it. The reason why this difficulty arises, in spite of the very large amplitude of our oscillations, can be understood from Fig. 4(a). In this figure, the $n_i=0$ and the $n_i=1$ oscillations overlap so that no really sharp structure can be associated with the $n_i=0$ oscillations. The sharp dip between the $n_i=1$ and the $n_i=2$ oscillations, on the other hand, occurs at a much lower field, so that it fades into the noise of the relatively high photon energy of 0.190 eV, and below this energy we can observe no sharp structures in the magnetoreflexivity at all. We therefore can only conclude that if there are carriers, their Fermi level does not greatly exceed 0.018 eV, which is the difference between the energy gap of 0.172 eV and the photon energy of 0.190 eV. Thus the Fermi level of 0.011 eV, measured by Priestley *et al.*¹ for the γ carriers, is consistent with our data.

Many of the other characteristics of the γ carriers are also consistent with our data. For example, Priestley *et al.* find that the Fermi surface for these carriers is a gently flared cylinder, with the long axis of the cylinder tilted about 11° away from the trigonal axis in the trigonal-bisectrix plane. The curvature of this band in the trigonal direction is therefore very small, which implies that the two pertinent bands interact weakly in the z direction. The cyclotron effective mass would therefore be very large for both bands when the magnetic field is parallel to the binary or bisectrix axes, which is consistent with our inability to observe any magnetoreflexion oscillations associated with these bands for these magnetic field orientations. Furthermore, the small band curvature would give us a very

²⁵ A critical point is defined as the k point for minimum energy separation between the valence and conduction bands. When the critical point is at a point of inversion symmetry, then the energy extrema for both bands occur at the critical point.

high density of states in the z direction which contributes to the large magnitude of our observed oscillations.

The measured band gap is also consistent with the model of Lin and Falicov,⁵ in that it can be identified with the spin-orbit splitting of the accidental degeneracy shown in Fig. 3. Since the spin-orbit splitting at the T point for arsenic was estimated to be between 0.24 and 0.32 eV by Falicov and Golin,²⁶ it seems reasonable to find a spin-orbit band gap of 0.172 eV at a point a small distance from T .

Finally, we note that the Lin-Falicov model predicts that the critical point for the transitions under consideration is along the Q axis in the Brillouin zone, which is an axis of low symmetry.²⁶ The symmetry is low enough, in fact, so that the cyclotron orbits corresponding to the magnetic energy levels in one band are not required to be concentric with the corresponding cyclotron orbits in the other band. One can show that the velocity matrix element for interband transitions between such states is not zero, for $\Delta n \neq 0$, and therefore justify the assumption that the $\Delta n = 0$ selection rule breaks down. This point is covered in more detail in the Appendix, where we actually calculate the velocity matrix elements for interband transitions at the Q point. It is shown that a breakdown in the selection rule $\Delta n = 0$ occurs if either the cyclotron orbits for the two bands are tilted with respect to each other, or if the energy extrema of the two bands are displaced, or more generally, if both mechanisms are simultaneously present.

IV. CONCLUSIONS

With the magnetic field along the trigonal axis, we have observed a series of oscillations in the magnetorefectivity of arsenic which seem to be associated with direct interband transitions between a pair of strongly interacting bands. The direct energy gap between the bands was measured to be 0.172 ± 0.003 eV, while the cyclotron effective mass at the band extremum was found to be 0.024 for magnetic fields parallel to the trigonal axis. One of the bands under discussion has been associated with the γ carriers, which have a cyclotron effective mass of 0.028 as measured by dHvA experiments.¹ This value is in excellent agreement with the cyclotron effective mass we have found.

The energy bands near the Fermi surface seem to be adequately described by the pseudopotential calculation of Lin and Falicov.⁵ This calculation also predicts that the extrema of the bands are at the Q point in the Brillouin zone, and we have been able to understand some of the observed peculiarities of the magnetoreflexion line shape and amplitude in terms of the low symmetry of the Q point.

An additional series of oscillations in the magnetorefectivity of arsenic has also been reported previously.⁶

These oscillations seem to be associated with direct interband transitions across a small, direct energy band gap of 0.346 eV between bands having either the T_2 and T_1' , or the T_1 and T_2' symmetries at the T point in the Brillouin zone. For magnetic fields perpendicular to the trigonal axis, the reduced cyclotron effective mass in this case was found to be 0.025, and there is some evidence that there may be a small pocket of carriers associated with one of the bands.⁶

In contrast to this experimental evidence, the band model of Lin and Falicov⁵ predicts that there are no small band gaps between bands of the above symmetries at T , and that there are no carriers at T at all. Their band model furthermore predicts that the γ carriers are only 0.07 a.u. away from T along the Q axis.²⁷ Although the magnetoreflexion experiment with H along the trigonal direction shows no inconsistencies with the Lin-Falicov band model at Q , the results with H along the binary and bisectrix directions are in direct conflict with the band model at point T , a short distance away. It would therefore be very interesting to recalculate the band structure of arsenic, and attempt to obtain a proper fit at both points in the Brillouin zone.

It also would be useful to further test the identification of the trigonal magnetoreflexion oscillations with the bands associated with the γ carriers. This could be done by measuring the dependence of the oscillations on the direction of the magnetic field more completely than was done in the present paper. If our identification is correct, a large orientation dependence should be observed.

ACKNOWLEDGMENTS

We would like to express our appreciation to S. Fischler, Mrs. K. Nearen, and W. Laswell for growing, cutting, and polishing the samples used. We are indebted to D. F. Kolesar for assistance in carrying out the measurements. We would also like to acknowledge stimulating discussions with Dr. G. Dresselhaus, Professor B. Lax, Dr. J. G. Mavroides, Professor G. W. Pratt, Jr., and Dr. Y. Shapira.

APPENDIX

In this Appendix, we calculate the velocity matrix elements for interband transitions between the two strongly interacting bands of Fig. 3(b). These bands are postulated to be nondegenerate parabolic bands with energy extrema lying along the TW or Q axes, which are axes of twofold rotation in the Brillouin zone of arsenic. We use the usual notation for the coordinate axis system, where the x axis is the axis of twofold rotation, the z axis is the trigonal axis, and the y (bisectrix) axis is the third member of the right-handed orthogonal set. We further assume that the two bands

²⁷ Here \mathbf{k} is expressed in atomic units or in units of $1/a_B$, where a_B is the Bohr radius.

²⁶ L. M. Falicov and S. Golin, Phys. Rev. **137**, A871 (1965).

interact very strongly in the x and y directions, and very weakly in the z direction. This assumption is justified by the results of the magnetoreflexion experiment as discussed in Sec. III. Finally, we only consider the case where the magnetic field is parallel to the trigonal axis, since this is the geometry of experimental interest.

In order to keep the calculation as simple as possible, the effects of spin will also be ignored. Since the band gap under consideration is produced by spin-orbit interaction, this assumption requires some justification. It can be justified by both an experimental and a theoretical argument. Experimentally, no fine structure is found on the magnetoreflexion spectra that could be attributed to spin splitting. Furthermore, the magnetoreflexion data seem consistent with a coupled two-band model like that encountered in bismuth,^{16,24} except that the $\Delta n=0$ selection rule does not apply. In the case of a strict two-band model with arbitrary spin-orbit coupling, it has been shown^{19,28} that spin has no effect on the resonant interband Landau-level transitions.

Since we have restricted ourselves to parabolic, spinless bands, we may now write ψ_j , the wave function for band j , as

$$\psi_j = F_j U_j, \quad (\text{A1})$$

where F_j is the envelope function and U_j is the core wave function at \mathbf{K}_0 , the point in the Brillouin zone from which we measure the crystalline momentum. Since there is no inversion symmetry at a general point along the twofold axis, the extrema of the two bands need not occur at the same point in the Brillouin zone. We therefore define \mathbf{K}_0 as the point on the twofold axis midway between the energy band extrema.

The envelope function is found by solving the single band, spinless effective-mass secular equation for band j ,

$$\{E_j^0 + (\boldsymbol{\pi} + \hbar \mathbf{k}_d \hat{x}) \cdot (\boldsymbol{\alpha}^j / 2m_0) \cdot (\boldsymbol{\pi} + \hbar \mathbf{k}_d \hat{x})\} F_j = E_j F_j, \quad (\text{A2})$$

where E_j^0 is the energy of band j at \mathbf{K}_0 , k_d is one-half the displacement between the band extrema, \hat{x} is the unit vector in the x direction, $\boldsymbol{\alpha}^j$ is the dimensionless reciprocal effective-mass tensor for band j , and

$$\boldsymbol{\pi} = \mathbf{p} - e\mathbf{A}/c. \quad (\text{A3})$$

Due to the twofold rotational symmetry about the x axis, it follows that

$$\alpha_{xy}^j = \alpha_{xz}^j = 0. \quad (\text{A4})$$

Furthermore, because the two bands interact strongly in the x and y directions,

$$\alpha_{xx}^u = -\alpha_{xx}^l \equiv \alpha_{xx} \quad (\text{A5})$$

and

$$\alpha_{yy}^u = -\alpha_{yy}^l \equiv \alpha_{yy}, \quad (\text{A6})$$

where $j=u, l$ for the upper and lower bands, respectively. Since the two bands interact weakly in the z direction, the remaining components of the effective-mass tensors for the two bands are unrelated, so that one expects the constant-energy surfaces for the two bands to be tilted with respect to each other in the yz plane.

Choosing the gauge where \mathbf{A} is parallel to the y axis, and solving the secular equation, we find

$$F_j = e^{ik_z z + ik_y y - ik_a x} \phi_n(x - x_j^0), \quad (\text{A7})$$

where $\phi_n(x - x_j^0)$ is the harmonic-oscillator function of index n centered at x_j^0 , and normalized over a unit volume in real space. In this function, the harmonic-oscillator center x_j^0 is

$$x_j^0 = \lambda^2 [k_y + k_z \alpha_{yz}^j / \alpha_{yy}^j], \quad (\text{A8})$$

where λ is the characteristic length:

$$\lambda = (\hbar c / eH)^{1/2}. \quad (\text{A9})$$

Using these wave functions, we may now calculate the velocity matrix elements for interband transitions between these states. Utilizing the slow spacial variation of the envelope functions, we make the usual approximation

$$\langle \psi_j | \mathbf{v} | \psi_{j'} \rangle = \langle F_j | F_{j'} \rangle \langle U_j | \mathbf{v} | U_{j'} \rangle. \quad (\text{A10})$$

We may then write

$$\langle \psi_j | \mathbf{v} | \psi_{j'} \rangle = \mathbf{v}_{jj'} \hat{I}(n, n', t, w), \quad (\text{A11})$$

where we have made the convenient definitions for the velocity matrix element between core states

$$\mathbf{v}_{jj'} \equiv \langle U_j | \mathbf{v} | U_{j'} \rangle, \quad (\text{A12})$$

and the overlap integral of the envelope functions

$$\hat{I}(n, n', t, w) \equiv \langle F_j | F_{j'} \rangle = \int_{-\infty}^{\infty} e^{2ik_a x} \phi_n(x - x_u^0) \times \phi_{n'}(x - x_l^0) dx. \quad (\text{A13})$$

The function $\hat{I}(n, n', t, w)$ is itself most conveniently written as a function of two dimensionless parameters t and w . In particular, the dimensionless parameter t describes the displacement of the band extrema along the k_x direction, and is related to k_d by

$$t = k_d \lambda (\alpha_{yy} / \alpha_{xx})^{1/4}. \quad (\text{A14})$$

The dimensionless parameter w describes the relative displacement of the centers of the conduction and valence band orbits along the k_y direction due to the relative tilt of the corresponding constant energy surfaces. Corresponding to the orbit-center displacement in the k_y direction, there is a real-space displacement between the harmonic-oscillator centers along the x direction, $x_l^0 - x_u^0$, which is related to w by

$$w = (1/2\lambda) (x_l^0 - x_u^0) (\alpha_{yy} / \alpha_{xx})^{1/4} = \xi \lambda k_z. \quad (\text{A15})$$

²⁸ P. A. Wolff, J. Phys. Chem. Solids **25**, 1057 (1964).

In Eq. (A15) the k_x dependence of w has been explicitly expressed by introducing the dimensionless parameter

$$\xi = \xi_u - \xi_l, \quad (\text{A16})$$

where

$$\xi_j = \frac{1}{2}(\alpha_{yy}/\alpha_{xx})^{1/4}(\alpha_{yz}^j/\alpha_{yy}^j). \quad (\text{A17})$$

These dimensionless parameters are introduced because it is convenient to work with the normalized harmonic-oscillator function $\theta_n(\nu)$ of the dimensionless argument ν , where

$$\nu = (\alpha_{xx}/\alpha_{yy})^{1/4}(x/\lambda) \quad (\text{A18})$$

and

$$\theta_n(\nu) = \pi^{-1/4}(2^n n!)^{-1/2} e^{-\nu^2/2} H_n(\nu), \quad (\text{A19})$$

in which $H_n(\nu)$ is the n th Hermite polynomial.²⁹ In order to evaluate the overlap integral, which can now be rewritten in terms of the dimensionless functions and variables as

$$\hat{I}(n, n', t, w) = \int_{-\infty}^{\infty} e^{2i\nu t} \theta_n(\nu+w) \theta_{n'}(\nu-w) d\nu, \quad (\text{A20})$$

we define a new complex variable of integration

$$q = \nu - it, \quad (\text{A21})$$

and a new complex displacement parameter

$$b = t + iw, \quad (\text{A22})$$

so that we may rewrite the integral as

$$\hat{I}(n, n', t, w) = \int_{-\infty}^{\infty} e^{-q^2 - bb^*} \frac{H_n(q+ib) H_{n'}(q+ib^*)}{(\pi^{2n+n'} n! n'!)^{1/2}} dq. \quad (\text{A23})$$

The integration can be taken along the real axis rather than along the line in the complex plane $\text{Im}q = -t$ because the integrand displays no singularities in the region enclosed by these two paths.³⁰ To evaluate this integral, we next note that the Hermite polynomial $H_n(q)$ contains terms no higher than the n th power in q , so that we may use a Taylor-series expansion to write the exact relation

$$H_n(q+ib) = \sum_{m=0}^n \frac{(ib)^m}{m!} \frac{d^m}{dq^m} H_n(q). \quad (\text{A24})$$

Furthermore, it can be easily established that

$$\frac{d^m}{dq^m} H_n(q) = \frac{2^m n!}{(n-m)!} H_{n-m}(q), \quad (\text{A25})$$

so that we may write

$$H_n(q+ib) = \sum_{m=0}^n \frac{(2ib)^m}{m!} \frac{n!}{(n-m)!} H_{n-m}(q). \quad (\text{A26})$$

Finally, from the orthonormality of the $\theta_n(q)$ functions, it follows that

$$\int_{-\infty}^{\infty} e^{-q^2} H_n(q) H_{n'}(q) dq = \pi^{1/2} 2^n n! \delta_{nn'}. \quad (\text{A27})$$

Using Eq. (A26) to expand the Hermite polynomials in Eqs. (A23) and (A27) to carry out the resulting integrals, we find

$$\hat{I}(n, n', b) = e^{-bb^*} (n! n'!)^{1/2} (i\sqrt{2}b)^{n-n'} \times \sum_{m=0}^n \frac{(-2bb^*)^m}{(n-n'+m)! (n'-m)! m!} \quad (\text{A28})$$

provided that $n' \leq n$. If this inequality is not satisfied, we can interchange n and n' and still use Eq. (A28). This interchange, however, introduces an error in the phase of the integral. On the other hand, physical quantities, such as the dielectric constant and conductivity, depend only upon the square of the magnitude of the velocity matrix elements, and therefore only involve the quantity $|\hat{I}|^2$. This phase is of no physical consequence; therefore, we replace the complex quantity b by its magnitude \hat{b} , and define the overlap integral function

$$I(n, n', \hat{b}) = e^{-\hat{b}^2} (n! n'!)^{1/2} (\sqrt{2}\hat{b})^{n-n'} \times \sum_{m=0}^n \frac{(-2\hat{b}^2)^m}{(n-n'+m)! (n'-m)! m!}. \quad (\text{A29})$$

We note from Eqs. (A14), (A15), and (A22) that \hat{b} is the normalized distance between the centers of those orbits in \mathbf{k} space, involved in the interband transition. Furthermore, we note from Eq. (A11) that the velocity matrix element for this transition is directly proportional to $I(n, n', \hat{b})$. Therefore, from Eq. (A29) we see that, as expected, when $\hat{b}=0$, the velocity matrix element is nonzero only for conventional $n=n'$ transitions. However, because of the low symmetry of a point along the TW axis, we would expect both t and w , and therefore \hat{b} to be nonzero. In that case, it is possible for $I(n, n', \hat{b})$, and also the velocity matrix element, to have a nonzero value even when $n \neq n'$. Therefore, the simple $\Delta n=0$ selection rule breaks down, as was assumed in Sec. III.

One may further extend this calculation, and use the velocity matrix elements derived here to calculate the field- and frequency-dependent conductivity of the material. A calculation of this type has been performed using the simplification that $t=0$, but $w \neq 0$.¹⁹ This simplification corresponds to the assumption that the critical point coincides with the energy extrema of the two bands. The results for this conductivity calculation are in qualitative agreement with experiment.

²⁹ A. Messiah, *Quantum Mechanics* (Wiley-Interscience Publishers, Inc., New York, 1961), Vol. 1, p. 491.

³⁰ R. V. Churchill, *Complex Variables and Applications* (McGraw-Hill Book Co., New York, 1960), p. 106.